agriculture

MDPI

Article

Vibrational Dynamics of Rice Precision Hole Seeders and Their Impact on Seed Dispensation Efficacy

Dongyang Yu [1,2], Feihu Peng [1,2], Zhihao Zeng [1,2], Minghua Zhang [1,2], Wenwu Yang [1,2], Ying Zang [1,2], Jianfei He [1,2], Yichen Huang [1,2], Yuguang Wu [1,2], Wenneng Zhong [1,2], Ziyou Guo [1,2], Jiawen Liu [1,2], Guanjiong Li [3], Xingmou Qin [3] and Zaiman Wang [1,2,*]

[1] Key Laboratory of Key Technology on Agricultural Machine and Equipment, South China Agricultural University, Ministry of Education, Guangzhou 510642, China; li33@stu.scau.edu.cn (D.Y.); ziyunle@stu.scau.edu.cn (F.P.); mh_z@scau.edu.cn (M.Z.); yangwenwu@scau.edu.cn (W.Y.); yingzang@scau.edu.cn (Y.Z.); hejianfei@scau.edu.cn (J.H.); huanyichen@stu.scau.edu.cn (Y.H.); 1070738779@stu.scau.edu.cn (Y.W.); zhongwenneng@stu.scau.edu.cn (W.Z.); liujiawen@stu.scau.edu.cn (J.L.)
[2] College of Engineering, South China Agricultural University, Guangzhou 510642, China
[3] Huangpu Innovation Research Institute, South China Agricultural University, Guangzhou 510715, China
* Correspondence: wangzaiman@scau.edu.cn

Abstract: This investigation considered the effects of both internal and external excitation vibrations on the efficacy of the seed dispenser in a rice precision hole seeder. Through comprehensive field tests, we analyzed vibrational characteristics during direct seeder operations and established a vibration seeding test bed for systematic examination of these effects. Time-domain analysis of the vibration data revealed a predominantly vertical vibration direction, with notably higher levels in sandy loam soil compared to clay loam. A correlation was observed between increased engine size and rotary ploughing speeds, as well as forward speed and elevated vibration amplitudes. Frequency domain analysis pinpointed the primary vibration frequency of the machinery within the 0–170 Hz range, remaining consistent across different operating conditions. Crucially, bench test results indicated that seeding accuracy and dispersion were significantly influenced by vibration frequencies, particularly within the 70–130 Hz range, where a decrease in accuracy and increase in dispersion were noted. A regression model suggested a complex, non-linear relationship between seeding performance and vibration frequency. These insights highlight the necessity for a robust mechanism to effectively address these vibrational impacts. This study paves the way for enhancing the operational efficiency of the rice precision hole seeder, aiming to achieve the design goals of minimized vibrations in the paddy power chassis.

Keywords: agricultural machinery; rice precision hole seeder; vibratory; sowing planter; seeding performance

check for updates

Citation: Yu, D.; Peng, F.; Zeng, Z.; Zhang, M.; Yang, W.; Zang, Y.; He, J.; Huang, Y.; Wu, Y.; Zhong, W.; et al. Vibrational Dynamics of Rice Precision Hole Seeders and Their Impact on Seed Dispensation Efficacy. *Agriculture* **2024**, *14*, 324. https://doi.org/10.3390/agriculture14020324

Academic Editor: Massimo Cecchini

Received: 17 January 2024
Revised: 8 February 2024
Accepted: 17 February 2024
Published: 18 February 2024

1. Introduction

Rice stands as the predominant grain crop in China, with mechanization proving particularly challenging in the realm of rice planting. Presently, China's mechanization rate for rice planting hovers around 50% [1–3]. To address this, China is actively pursuing the development of mechanized precision direct seeding technology as a streamlined, light-cultivation approach to rice cultivation [4–6]. This technology holds promise for minimizing seed loss and improving sowing uniformity [7,8], thereby positively influencing early-stage rice development and overall yields [9–11]. Despite its theoretical advantages, practical implementation faces challenges [12,13]. During the operation of precision rice hole-drilling machines, uneven terrain induces complex vibrations, impacting seed dispensing stability and potentially leading to inaccuracies in seed dispersal. Consequently, this affects the crop growth performance and final yield [14–16].

In recent years, both domestic and international studies have considered the vibration characteristics of planting machines and their repercussions for crop yields. Liao Yitao et al. [17] investigated the relationship between the vibration characteristics of a pneumatic oilseed rape planter and the performance of its seed displacer, revealing both beneficial and detrimental effects. Wang Qi et al. [18] analyzed a mathematical model of vibration for a no-till precision planter, proposing measures to mitigate vibration, such as adjusting the forward speed and optimizing machine structure. Gu Chunli et al. [19] scrutinized the vibration characteristics of the planter frame using ANSYS Workbench software, identifying reasons for the deformation response. Xu Lizhang et al. [20] conducted vibration tests on a domestic tracked combine harvester in the field, offering insights into primary and secondary factors contributing to machine vibration. Internationally, Far et al. [21] and MF et al. [22] studied high-speed no-tillage seeding, discovering that vibration significantly affected the seeders. Niyamapa and colleagues [23] found that using a vibratory deep loosening machine applies force horizontally and vertically. Meanwhile, Vu-Quoc and colleagues [24] utilized a ball to construct a three-dimensional model of soybeans, conducting drop and compression tests to determine soybeans' mechanical characteristics. Min et al. [25] established that specific vibration frequencies and amplitudes do not affect the vacuum suction in seed boxes. While extensive research has been conducted on seed dispensers design for various seeder models, investigations into the vibration characteristics of seeders during operation, especially pneumatic seeders, remain limited. Previous studies have optimized structural parameters by establishing surface data models, but the rice precision hole seeder has not been studied. Therefore, an examination of seeding quality under vibrational conditions was warranted.

In this investigation, we conducted an exhaustive analysis of the vibrational characteristics inherent to a direct-seeding apparatus for rice, under conditions that closely mimicked actual agricultural scenarios. This was achieved through a combination of controlled laboratory simulations and extensive field testing. By comparing the outcomes of bench-scale tests with real-world experiments, we systematically evaluated how mechanical vibrations influenced the performance of the seed dispensing mechanism across varying operational speeds and under different soil conditions. The core contribution of our study is the development of precise, quantitative parameters for vibration control. These parameters are essential for the design and operation of a direct seeder equipped with precision apertures, aimed specifically at rice agriculture. By integrating these parameters, we significantly enhanced the machine's operational efficiency and seed placement accuracy. The enhancements delineated in our research are pivotal for realizing unprecedented levels of efficiency and precision in rice cultivation practices, thereby addressing some of the most pressing challenges in modern agriculture.

2. Seeder Structure and Working Principle

The configuration of the rice precision hole seeder, illustrated in Figure 1, comprises a frame, a seeding ditch and water storage ditch ditching device, horizontal and elevation profiling mechanisms, a power transmission device, a seeding device, and a hydraulic lifting mechanism. The sowing and seeding devices, along with furrowing device 1, are securely affixed to frame 8. The bearing seat of the horizontal profiling mechanism 4 is mounted on the same frame 8, with one end fixed to hitching bracket 5. This bracket 5 connects to the power chassis through the universal transmission shaft, which, in turn, is linked to the PTO power rotation device 6. The power chassis supplies the necessary power for walking, lifting, and sowing. The machine tool is suspended from the power chassis with the assistance of hydraulic oil cylinders and lifting frames situated on the parallel four-bar lifting frame. Concurrently, hydraulic cylinders and lifting frames positioned at the rear of the power chassis support the implement.

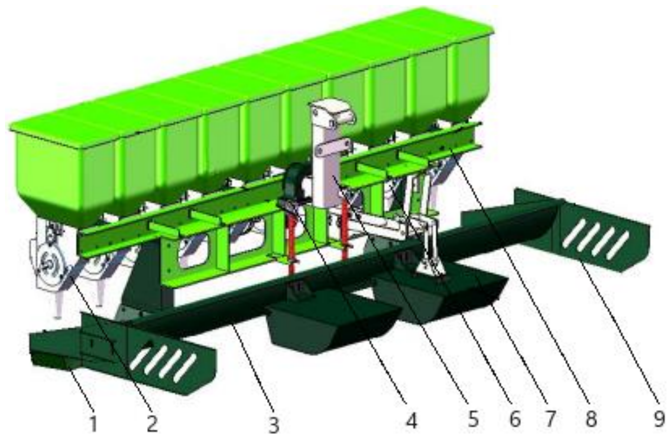

Figure 1. The structure of the rice precision hole seeder. 1. Furrowing device. 2. Seed distributor. 3. Slide plate. 4. Horizontal profiling mechanism. 5. Hitching bracket. 6. PTO power rotation unit. 7. Elevation profiling mechanism. 8. Frame. 9. Lateral panels.

During operation, the operating handle of the power chassis is set to the insert and plant gear, prompting the hydraulic cylinder to unload. Subsequently, the machine descends under its own weight, and the slide plate 3 remains in close proximity to the mud surface, guided by the actions of the elevation profiling mechanism 7 and the horizontal profiling mechanism 4. The seeding furrow opener 1 and the water storage furrow opener 1 are then pressed into the soil, creating furrows for seeding and water storage as the machine advances. Simultaneously, the seed distributor 2, driven by the PTO power rotation unit 6, deposits seeds into the sowing furrow through perforations. Two lateral panels 9, designed to block mud, serve as barriers to prevent water and mud from infiltrating into the seeded region.

3. Seeder Vibration Characteristics Testing and Analysis

3.1. Equipment

The experiment used a Yanmar VPG6G power chassis from the Japanese company Yanmar (Osaka, Japan) for rice transplanting. It was equipped with a 2BDXZ-10CP (20) precision hole seeder by South China Agricultural University (Guangzhou, China) specifically designed for rice sowing. Table 1 provides detailed information on key parameters [26].

Table 1. Parameters related to vibration test work equipment.

Device Name	Items	Parameter Value
Yanmar VPG6G rice transplanter power chassis	Power Chassis Weight (m_a, kg)	720
	Operating speed (v, km·h^{-1})	0~5.3
	Rated engine power (P, kW)	10.3
	Wheelbases (L, mm)	1050
	Front wheelbase (l_r, mm)	1220
	Rear wheelbase (l_f, mm)	1200
2BDXZ-10CP(20) rice precision hole seeder	Seeder size (L × W × H, mm)	1050 × 2080 × 500
	Seeder weight (m_b, kg)	185
	Working width (mm)	2000
	Number of rows sown	10
	Row spacing (cm)	20
	Distance between holes (cm)	10~20 adjustable
	Seeding rate (kg·hm^{-2})	22.5~75 (3~10 grain/cavity adjustable)

The vibration analysis system was employed to evaluate the 2BDXZ-10CP(20) rice precision hole seeder, utilizing the MCC DAQ data acquisition system for data collection. The setup incorporated a USB-1608G multifunctional data acquisition device and a CT1010SLFP piezoelectric tri-axial acceleration transducer from Shanghai CHENGTEC (Shanghai, China), enabling the comprehensive assessment of vibrational characteristics. The evaluations were conducted under a variety of terrain conditions to ensure the robustness of the seeder's performance. Key performance metrics of the instrumentation, critical for understanding the precision and reliability of the measurements, are systematically presented in Table 2.

Table 2. Main performance parameters of the test instrument.

Device Name	Items	Parameter Value
CT1010SLFP Piezoelectric Triaxial Acceleration Sensor	Range (g)	±50
	Frequency response (Hz)	0.5~8000
	Degree of sensitivity (mV·g^{-1})	100
	Lateral sensitivity (%)	<5
USB-1608G Multi-function Data Acquisition Instrument	Channel number	16
	Maximum sampling rate (kS·s^{-1})	500
	Distortion (%)	<0.5

3.2. Test Conditions and Methods

The vibration characteristic test was conducted in July 2023 at the Teaching and Research Base of South China Agricultural University and the Research Base of Dajisha, both situated in Guangzhou City, Guangdong Province. The soil type in the test field consisted of clay loam and sandy loam, and the vibration test site is depicted in Figure 2. Relevant field parameters outlining its characteristics are detailed in Table 3.

(**a**) (**b**)

Figure 2. Seeder vibration test under different field soil-type conditions: (**a**) clay loam field, (**b**) sandy loam field.

Table 3. Parameters related to field characteristics.

Field Type	Items	Parameter Value
Clay loam field	Soil moisture content of the subsoil (%)	37.6
	Soil cohesion (kPa)	2.83
	Permissible soil weight (g·cm^{-3})	1.81
Sandy loam field	Soil moisture content of the subsoil (%)	31.3
	Soil cohesion (kPa)	2.56
	Permissible soil weight (g·cm^{-3})	1.75

Various fields with distinct characteristics and operational speeds were carefully selected for the comprehensive analysis of the vibration properties inherent to the rice precision hole seeder. Before testing, both paddy fields featuring clay loam and sandy loam characteristics underwent leveling and compaction processes. The testing material comprised Huanghuazhan Indica rice seeds, possessing a water content of 23.5%.

Figure 1 illustrates the structural configuration of the rice precision hole direct seeding machine, which features a ten-row seeding assembly aligned symmetrically along the central axis of the frame. To capture the dynamic vibrational behavior associated with the operational mechanics of the machine, dual tri-axial acceleration sensors were strategically positioned within the first and fifth rows of the seeding apparatus. These sensors were oriented to measure accelerations along three principal axes: the longitudinal axis, corresponding to the machine's forward motion; the vertical axis, aligned with gravitational pull; and the lateral axis, perpendicular to the other two. The precise locations of these sensors are depicted in Figure 3, providing a clear visual reference of their placement in relation to the machine's geometric layout. This arrangement facilitated a comprehensive analysis of the vibrational forces exerted during the direct seeding process, enabling a nuanced understanding of the machine's operational dynamics.

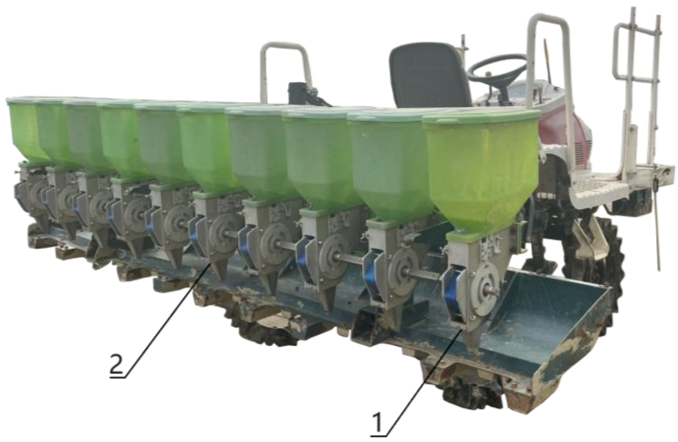

Figure 3. Acceleration sensor test point location. 1. First row of seeders. 2. Fifth row of seeders.

During the investigation, the power chassis of the machinery was initially positioned in the planting configuration. Six distinct speeds were selected for a comprehensive vibrational analysis: stationary (0 m/s, unloaded), and operational speeds of 0.31 m/s, 0.61 m/s, 0.83 m/s, 1.13 m/s, and 1.27 m/s. The MCC DAQ data acquisition system was meticulously set to perform continuous sampling at a rate of 2000 Hz, translating to a sampling interval of 0.5 ms. The initiation of testing was contingent upon stabilization of the vehicle's speed.

The experimental design included 36 distinct test groups, stratified by two types of characteristic fields, six varying speeds, and three iterations for each condition, ensuring a robust statistical dataset. Selection of test segments was executed randomly to avoid bias, with the stipulation that the machinery maintain a linear trajectory throughout each 30 s evaluation period. The vibrational analysis employed a MCC DAQ system, which facilitated continuous data acquisition, capturing the dynamic response of the machinery under varied operational conditions.

3.3. Analysis of Vibration Characteristics

3.3.1. Time-Domain Characteristic Analysis

The time-domain signals obtained from the fifth seed dispenser for the three axes of the direct seeder are illustrated in Figure 4. The direct seeder, operating at a speed of 1.13 $m \cdot s^{-1}$, was engaged in a clay loam soil field. Notably, the amplitude of the time-domain signals in the Y-axis surpassed that in the X-axis and Z-axis. This observation implies that the seeder experienced heightened vibration when operating perpendicular to the ground surface. Consequently, future investigations will concentrate on discerning the vibration characteristics in the vertical direction, specifically along the Y-axis.

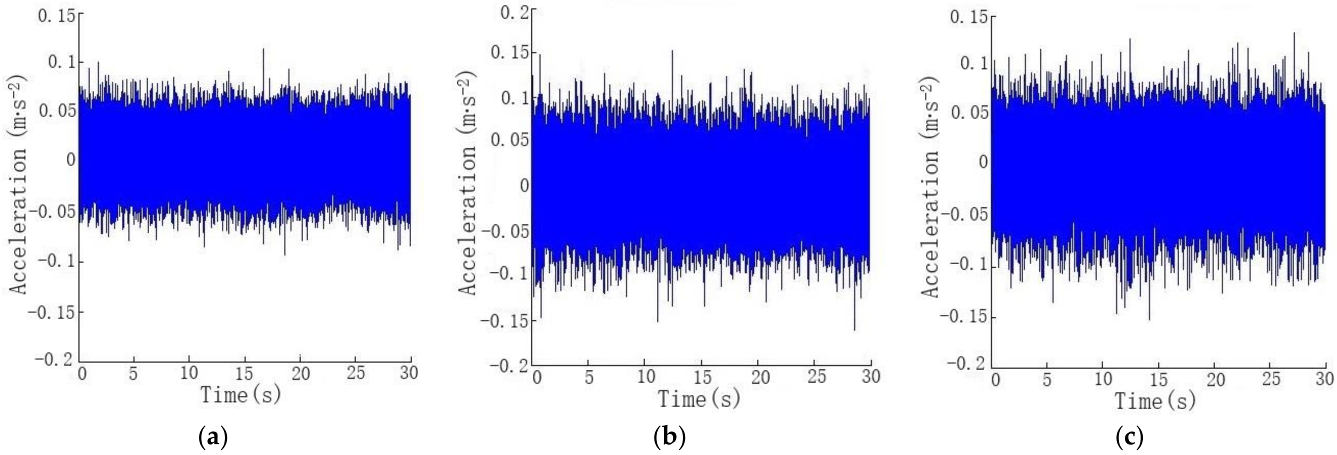

Figure 4. Vibration time-domain signals from the fifth seed discharger of a direct-driven machine operating at a speed of 1.13 m/s in a clay loam soil field: (**a**) forward direction (X-channel), (**b**) vertical direction (Y channel), and (**c**) swing direction (Z channel).

The evaluation of vibration amplitudes during the operational deployment of the direct seeder was quantified using the root mean square (RMS) value of vibration acceleration, a standard metric for assessing vibrational intensity [27]. Vibrations were observed to emanate from both the engine and the power take-off (PTO) during operation, as highlighted by the results obtained under no-load conditions (0 m/s). The experimental framework encompassed field tests across two soil variants: clay loam and sandy loam.

Figure 5 delineates the RMS acceleration values of vertical vibrations detected for both the initial and fifth rows of seeders, across a range of operational velocities. It is evident from the data that the actuation of the direct seeder markedly intensified the RMS values relative to the quiescent, unloaded state. Furthermore, a direct correlation was observed between the RMS values and the seeder's forward velocity under consistent soil conditions. Notably, within identical soil and speed parameters, the RMS values recorded at the fifth row of seeders consistently exceeded those measured at the first, suggesting a spatial variation in vibrational impact across the seeder's configuration.

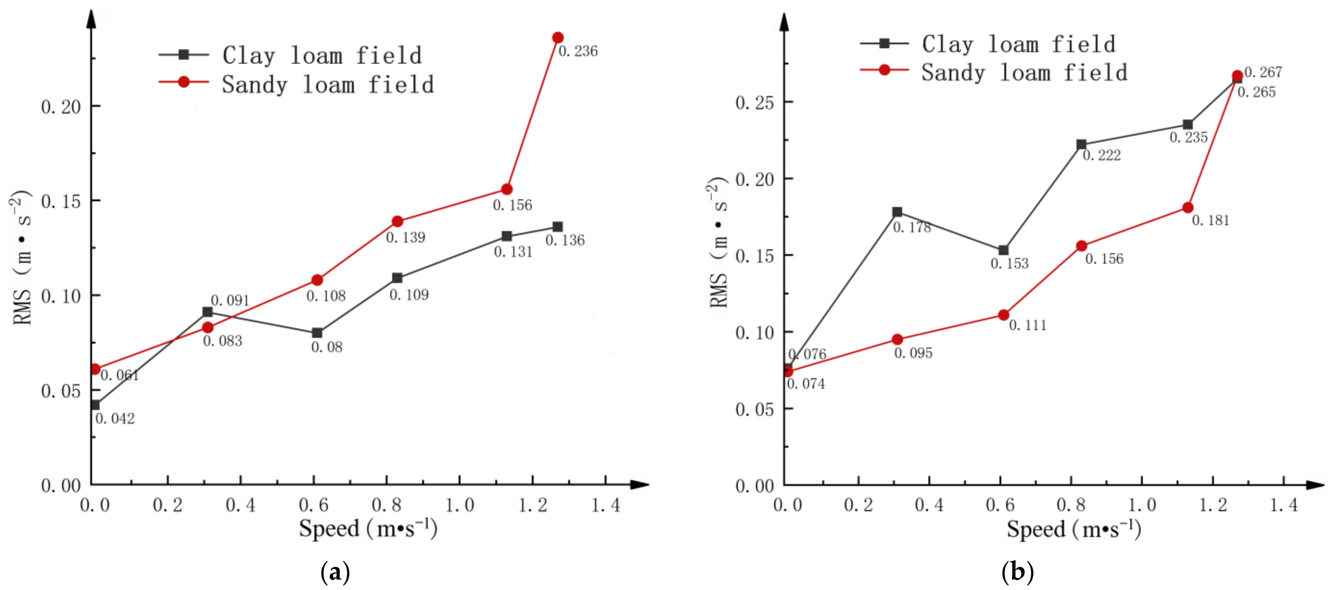

Figure 5. Root mean square values for vibration acceleration were obtained for the initial and fifth seed rowers of the direct seeding equipment: (**a**) first row of seeders, (**b**) fifth row of seeders.

A notable discrepancy was observed between the RMS values of the initial and fifth seeders of the direct seeder, evident across its operation. The RMS values of the first-row seeder in sandy loam fields at the same operating speed were slightly higher than those in clay loam fields. Meanwhile, the RMS values of the fifth-row seeder in sandy loam fields were often lower than those in clay loam fields. The RMS of the first-row seeder in clay loam fields was the lowest, whereas that of the fifth-row seeder in the same fields was the highest. Similarly, the RMS of the first-row seeder in sandy loam fields was the lowest, and that of the fifth-row seeder in clay loam fields was the highest.

The vibration time-domain signal amplitude of the direct seeder during sandy loam soil field operations at the medium level was primarily associated with engine speed, rotary plowing rotational speed, equipment forward speed, and seeding ground conditions. The performance of the fifth-row seeder was comparable.

The RMS measurements in the paddy field environment indicated that the first row of the direct seeder had an average RMS value of 0.109 $m \cdot s^{-2}$, while the fifth row registered an average RMS value of 0.211 $m \cdot s^{-2}$. Consequently, the vibration intensity of the fifth row of the direct seeder significantly exceeded that of the first row under the operational conditions of the clay loam soil field. In the sandy loam field environment, the direct seeder's first position had an average RMS value of 0.144 $m \cdot s^{-2}$, and the fifth position had an average RMS value of 0.162 $m \cdot s^{-2}$. Although the vibration acceleration at both positions in the sandy loam field was higher than that in the clay loam field, the difference between the first and fifth seeder positions of the direct seeder was relatively smaller in the sandy loam soil field.

In both operating environments, it was evident that the vibration acceleration of the direct seeder's fifth row was higher than that of the first row. The average RMS value for the first-row seeder positions was 0.127 $m \cdot s^{-2}$, whereas that of the fifth row was 0.186 $m \cdot s^{-2}$. These results indicate that the vibration acceleration of the direct seeder's fifth row was generally higher in both the clay loam and sandy loam soil field operating environments. The various environments significantly impacted the vibrational acceleration of the power chassis and the attached rice direct seeder, with the vibration level being higher in the sandy loam field than in the clay loam field. This discrepancy may be attributed to differences in soil texture, moisture content, and surface roughness. The fifth row of seeders on the direct seeder experienced elevated levels of vibration acceleration compared to the first seeder row, likely due to its proximity to the power chassis implement lifting hitch and its central position in mechanical transmission and force transfer, making it subject to greater forces and vibrations.

3.3.2. Frequency Domain Characteristic Analysis

The field-measured vibration signals of the direct seeder underwent Fourier transform using MATLAB software, version 2021, to reveal their spectral characteristics. Table 4 presents the vibration frequencies of the first three orders of the seeders' vibration signals in diverse operating environments, encompassing clay loam and sandy loam fields. Remarkably, at the same position on the seeder row, the power chassis equipped with a live broadcasting machine exhibited similar vibration frequency distribution signals for the first three orders in both clay loam and sandy loam fields, despite variations in forward speed. This consistency implies that the primary vibration frequency distribution of the seeder row remained stable across the various operating environments and was not significantly influenced by vibration excitation. Shui Tian's research determined that the distribution density of the power spectrum for the excitation frequency plays a pivotal role in governing the power chassis engine's combustion work. Furthermore, the distribution density of the power spectrum for the excitation frequency induced by road conditions constitutes a significant contributing factor.

Table 4. Vibration frequency and peak amplitude of each measurement point under different working conditions.

		First Row of Seeders			Fifth Row of Seeders		
		First Order Frequency (Hz)	**Second Order Frequency (Hz)**	**Third Order Frequency (Hz)**	**First Order Frequency (Hz)**	**Second Order Frequency (Hz)**	**Third Order Frequency (Hz)**
Clay loam field	0 m·s^{-1}	12.73	152.6	38.18	114.2	8.18	76.29
	0.31 m·s^{-1}	3.73	136.7	34.33	106.1	3.73	52.98
	0.61 m·s^{-1}	2.51	131.2	59.66	119.3	2.525	48.62
	0.83 m·s^{-1}	4.3	132.8	46.65	131.7	3.273	45.58
	1.13 m·s^{-1}	4.13	135.1	46.07	139.4	4.57	46.34
	1.27 m·s^{-1}	5.32	155.5	77.85	155.5	4.715	52.2
Sandy loam field	0 m·s^{-1}	12.76	153.1	38.27	114.8	12.87	76.57
	0.31 m·s^{-1}	4.28	136.3	32.52	146.4	3.46	51.21
	0.61 m·s^{-1}	4.07	109.8	24.13	113.9	2.52	54.96
	0.83 m·s^{-1}	3.87	130.3	46.07	130.4	2.6	47.47
	1.13 m·s^{-1}	4.33	139.3	34.3	142.6	3.82	50.27
	1.27 m·s^{-1}	5.58	128.6	46.3	128.5	2.35	52.35

The vibration test on the first row of seeders for the direct broadcasting machine revealed that the vibration frequencies of the first three peaks were approximately 4 Hz, 40 Hz, and 130 Hz. Concurrently, the test on the fifth row confirmed that the vibration frequencies of the first three peaks were roughly at 3.5 Hz, 50 Hz, and 130 Hz. Both the first and fifth rows of seeders underwent testing under identical operating conditions. The results indicate that the peak frequency, hovering around 130 Hz, closely corresponds to twice the engine excitation frequency. Similarly, the peak frequency around 40 Hz aligns with twice the excitation frequency of the PTO rotary ploughing device. Lastly, the peak frequencies at approximately 4 Hz and 3.5 Hz coincide with the excitation frequency generated by road conditions.

Figures 6 and 7 display three-dimensional spectrograms illustrating various soil operating environments of the paddy power chassis attached to the direct seeder at different seeder positions. Notably, the density of the power spectrum distribution, driven by the combustion of the engine mixture in the paddy power chassis, emerges as the dominant factor. Distinct data distributions are observed for the different row seeder test locations in clay loam and sandy loam fields, with significant variations in frequency and peak distributions at different vehicle speeds. Notably, the power spectral density peak of the fifth row seeder in the direct seeder was more pronounced in both operating environments. While the trend of the power spectral density remained consistent for the same row seeder test position in both operating environments, the peak in the sandy loam field operation exhibited greater variability than in the clay loam field operation.

Analysis of the predominant vibrational frequency of the seed dispenser across various operational speeds demonstrates a discernible pattern, wherein the peak of the acceleration power spectrum escalated concomitantly with an increase in travel speed. Investigation into the distribution of the main vibrational frequencies under diverse operational conditions highlighted that the pivotal determinants of frequency distribution within the seed dispenser of the direct broadcasting machine were chiefly the engine speed of the paddy power chassis and the vibrational stimuli emanating from the road surface across the different agricultural terrains.

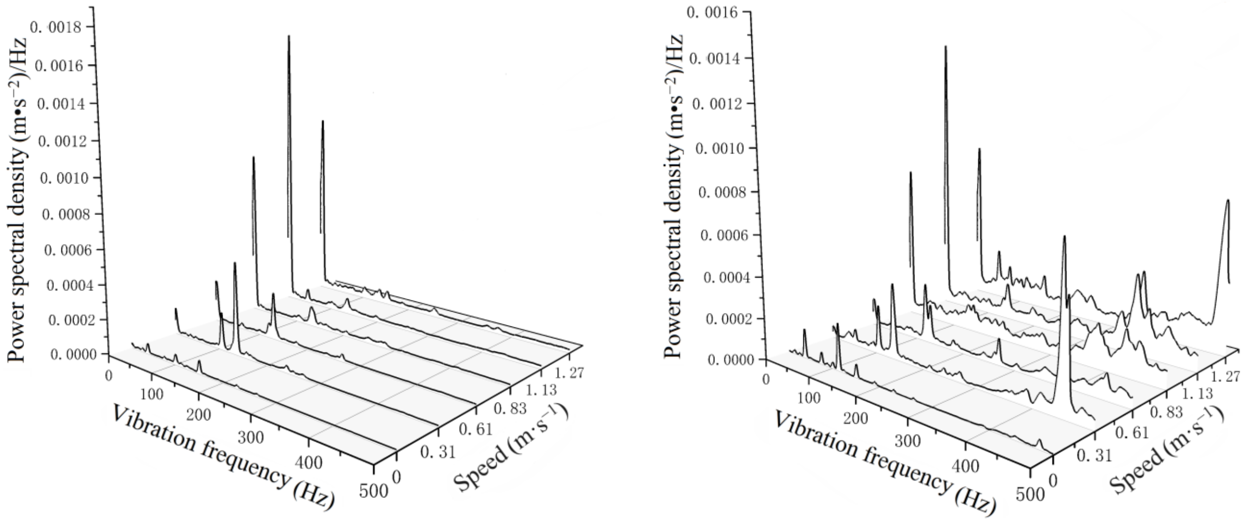

(**a**) (**b**)

Figure 6. Three-dimensional spectrograms of acceleration for different seed dischargers operating in a clay loam field: (**a**) first row of seeders, (**b**) fifth row of seeders.

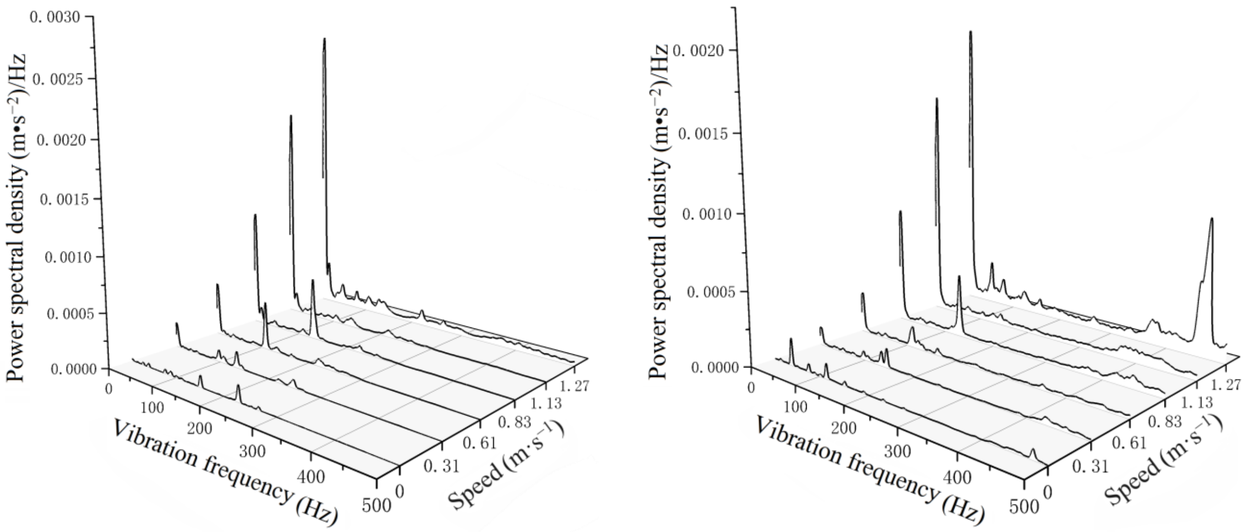

(**a**) (**b**)

Figure 7. Three-dimensional spectrograms of acceleration for different seed dischargers operating in a sandy loam field: (**a**) first row of seeders, (**b**) fifth row of seeders.

4. Bench Tests on the Effect of Seeder Performance

4.1. Test Conditions and Methods

To evaluate the effect of seeder vibration on the performance of the seed discharger, we used a HD-G809-5 six-degree spatial vibration tester from Haida International Equipment (Suzhou, China) as a carrier for the seed test bed. The vibration test bed's overall structure is depicted in Figure 8. The seed discharger, along with its supporting motor, was securely installed in six degrees of spatial orientation on the vibration table, to replicate the field vibration operating conditions. The supporting motor, acting in lieu of the power chassis PTO, drove the seed discharger's operation. The conveyor belt, simulating the forward movement of the direct broadcast machine, facilitated the discharge of rice seeds onto an oiled surface. This conveyor belt adopts equipment from JIALIAN Automation Equipment Co. (Shenzhen, China). An image acquisition camera, provided by MSHiWi Technology Co. (Shenzhen, China), captured visual data of the adhered seeds on the conveyor belt. Essential parameters of the experimental setup are detailed in Table 5.

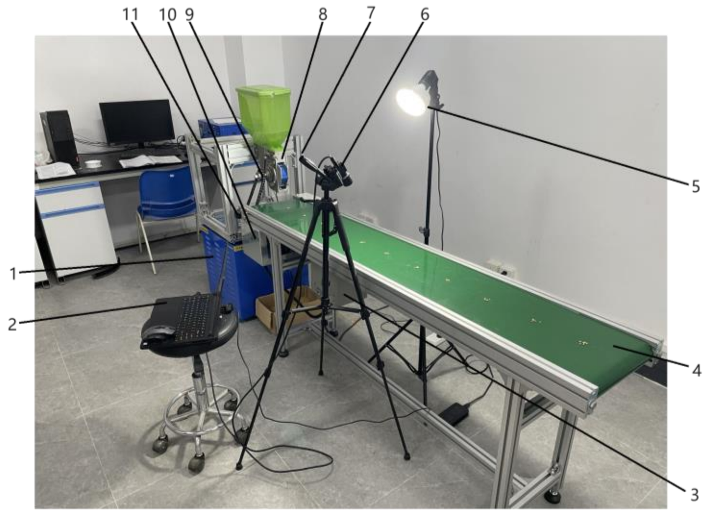

Figure 8. Seeder vibration test stand. 1. Six-degree spatial vibration tester. 2. Computer. 3. Conveyor controller. 4. Conveyor belts. 5. Fill light. 6. Image acquisition camera. 7. Seeder holder. 8. Seeder. 9. Seeder sprocket. 10. Motor controller. 11. Electrical machinery.

Table 5. Functional parameters of the laboratory bench.

Equipment Name	Item	Parameter
Conveyor belts	Conveyor belt (L × W, cm)	300 × 30
	Conveyor belt material	PVC
	Conveyer speed (m·s^{-1})	0~1.3
Image acquisition camera	Camera model	AF16V20
	Pixel	16 million
	Resolution	4656 × 3496
	Focusing method	Automatic
	Zooming	Autofocus
	Angle	Wide Angle 95°, Viewing Angle 65°
Six-degree spatial vibration tester	Model	HD-G809-5
	Direction of vibration	Triaxial vibration
	Size (L × W × H, mm)	500 × 550 × 500
	Weight-bearing capacity (kg)	0~100
	Acceleration interval (g)	0~15
	Sweep Range (Hz)	0.5~600
	Vibration waveform	Sine wave

In this study, Hwanghwa Cham rice seeds characterized by their elongation and indica variety with a moisture content between 22.8% and 23.7% were subjected to pre-germination until they exhibited a white hue at the sprouting stage. A 2BDXZ-10CP (20) rice precision hole seeder seed dispensing mechanism, a versatile unit capable of manual adjustment to accommodate varying seed sizes through selectable hole dimensions, facilitated the dispensation of seeds at two distinct rates: 3–6 grains per hole and 7–10 grains per hole. This adaptability allowed for the precise control of sowing densities to suit diverse agricultural requirements.

The vibrational frequencies selected for evaluation spanned from 0 to 170 Hz, as informed by the frequency domain analysis of the direct seeder, detailed in Table 4. These frequencies were segmented into three categories for analysis: low-frequency (0–60 Hz), medium-frequency (70–130 Hz), and high-frequency (140–170 Hz) vibrations, to comprehensively understand the impact of vibrational forces across the spectrum.

For the purposes of visual documentation, an image acquisition system comprising a camera interfaced with a computer via USB was employed. The camera, set to automatic shutter release, was positioned 205 mm above the conveyor belt, equipped with a 4 mm lens yielding a field of view measuring 355 × 200 mm. Image capture intervals were synchronized with the conveyor's speed at 1.5 s intervals to ensure distinct, non-overlapping images of the seed discharge process.

Prior to each test series, the shaking table's control settings were meticulously calibrated to achieve the desired vibrational conditions. The conveyor speed was fixed at 1 m/s to achieve a consistent seed spacing of 12 cm. Following adjustments to ensure the conveyor's smooth operation, the motor was regulated to maintain a rotation speed of 60 rpm and a sowing height of 180 mm, facilitating the precise deposition of seeds onto the oiled surface of the seedbed conveyor for subsequent image-based analysis.

In this investigation, seeding accuracy and dispersion were selected as the primary metrics for evaluating the performance of seed dischargers [28,29]. Seeding accuracy (μ) was quantitatively defined as the proportion of seeds accurately deposited into the designated seed slot relative to the overall count of seeds dispensed. Given the dimensions of the rice hole seeder's seed slot at 35 mm and the width of the seeding experimental stand's conveyor belt set at 200 mm, meticulous calibration of the camera's positioning enabled the mapping of seeding strip width to image pixel dimensions, as illustrated in Figure 9. Consequently, seeding accuracy within this context was articulated as the fraction of seeds captured within the pixel range of 186 to 264 along the y-axis of the image, compared to the aggregate seed count depicted. Mathematically, seeding accuracy (μ) was represented by the following formula:

$$\mu = \frac{m_1}{m_2} \tag{1}$$

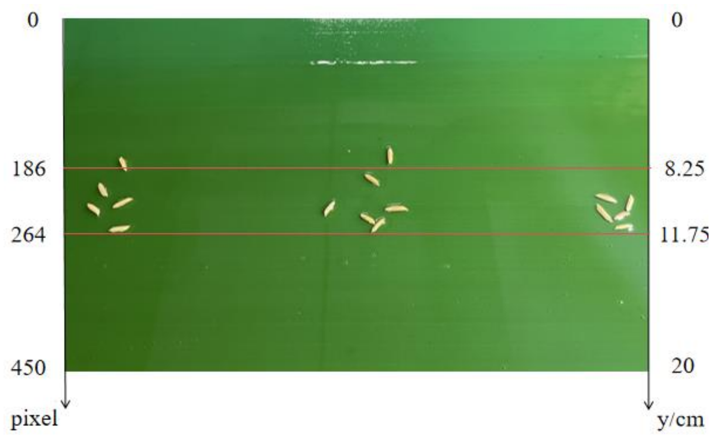

Figure 9. Correspondence between seeding slot width and image pixels.

In the equations presented, m_1 denotes the number of seeds located within a specified pixel range in the captured image, whereas m_2 accounts for the total seed count observed within the entire image. A higher value of μ (seeding accuracy) signifies a more precise alignment of seeds within the designated seed slot, thereby enhancing the overall precision of the seeding process.

The variable V (sowing dispersion) quantifies the variability in the spatial distribution of seeds deposited into the seed slot, which has significant implications for the uniformity of crop emergence and growth. Optimally, a reduced dispersion is preferable, as it supports a more uniform root system development in hole-sown rice crops. In this study, sowing dispersion was specifically defined as the variability in the placement of seeds across the width of the seed slot. This was assessed through continuous image capture by an image acquisition camera focused on the seed conveyor belt, where seeds positioned within the y-direction pixel range of 186 to 264 were analyzed. The analysis involved recording the distance (y_i) between each seed and a reference line, corresponding to the y-direction pixel value of 186, to calculate V, the measure of sowing dispersion.

$$
\begin{aligned}
\overline{y} &= \frac{\sum_{i=1}^{n} y_i}{n} \\
S' &= \sqrt{\frac{\sum_{i=1}^{n} (y_i - \overline{y})^2}{n}} \\
V &= \frac{S'}{\overline{y}}
\end{aligned}
\tag{2}
$$

where $\overline{y}$ is the mean value of y_i; S' is the standard deviation of y_i; n is the number of seeds falling within pixels 186~264 in the y-direction. The larger the value of V, the higher the degree of dispersion of the sowing.

4.2. Analysis of Test Results

The correlation between seed dispenser sowing accuracy and sowing dispersion curves across different frequencies is depicted in Figure 10. Within the low-frequency interval, the seeding accuracy of small holes averaged 95.46%, declining to 94.38% in the mid-frequency interval, and slightly recovering to 95.71% in the high-frequency interval. Similarly, the seed dispenser's large hole sowing accuracy mirrored this trend, averaging 95.34%, 94.25%, and 95.08% in the low, mid, and high-frequency intervals, respectively. Conversely, the average dispersion of seeding for large holes increased from 19.49% in the low-frequency interval to 20.81% in the medium-frequency interval and slightly decreased to 20.72% in the high-frequency interval. The average dispersion of small hole sowing followed a similar pattern, registering 19.55%, 20.85%, and 20.66% in the low, mid, and high-frequency intervals, respectively.

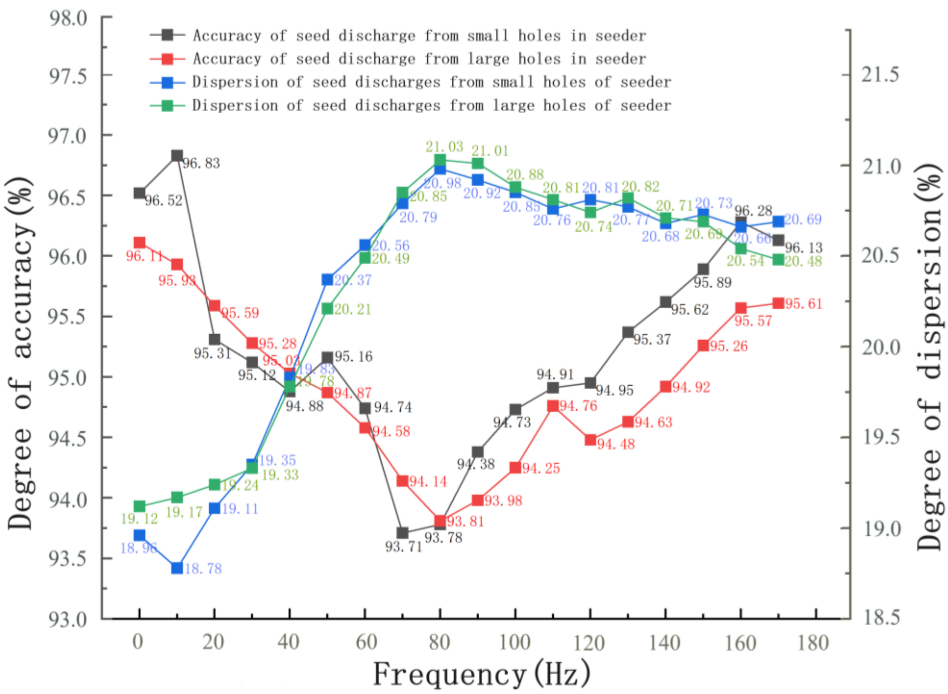

Figure 10. Relationship between seeding accuracy and dispersion curves of seed dischargers at different frequencies.

The observed trend highlights the significant impact of vibration frequency on the seeding accuracy and dispersion of the planter seeder. Particularly in the mid-frequency vibration interval, the decrease in seeding accuracy and increase in seeding dispersion may have stemmed from mechanical instability and resonance effects induced by vibration. As the frequency further increased to the high-frequency interval, the accuracy recovered, while the increasing trend of dispersion slowed down or even decreased, possibly due to the diminishing effect of high-frequency vibration on the mechanical structure. Correlation analysis indicated a moderate negative correlation (−0.54) between the small hole seeding accuracy and dispersion, and a strong negative correlation (−0.74) for large holes. The negative correlation between seeding accuracy and dispersion, particularly pronounced for large holes, implies that increased accuracy led to a reduced seed dispersion and vice versa. This relationship can be attributed to the effective control of seed dispenser filling and discharge during stable operation, resulting in reduced seed dispersion at the time of landing.

Linear and quadratic regression analyses, presented in Figure 11, further explored the relationship between the vibration frequency of the seed discharger and sowing accuracy and dispersion. The complex relationship observed suggests a non-linear correlation, emphasizing that the variation in seed discharge performance with vibration frequency was influenced by multiple factors, including the response characteristics of the direct seeder's mechanical structure and the intricate conditions of the power chassis operation.

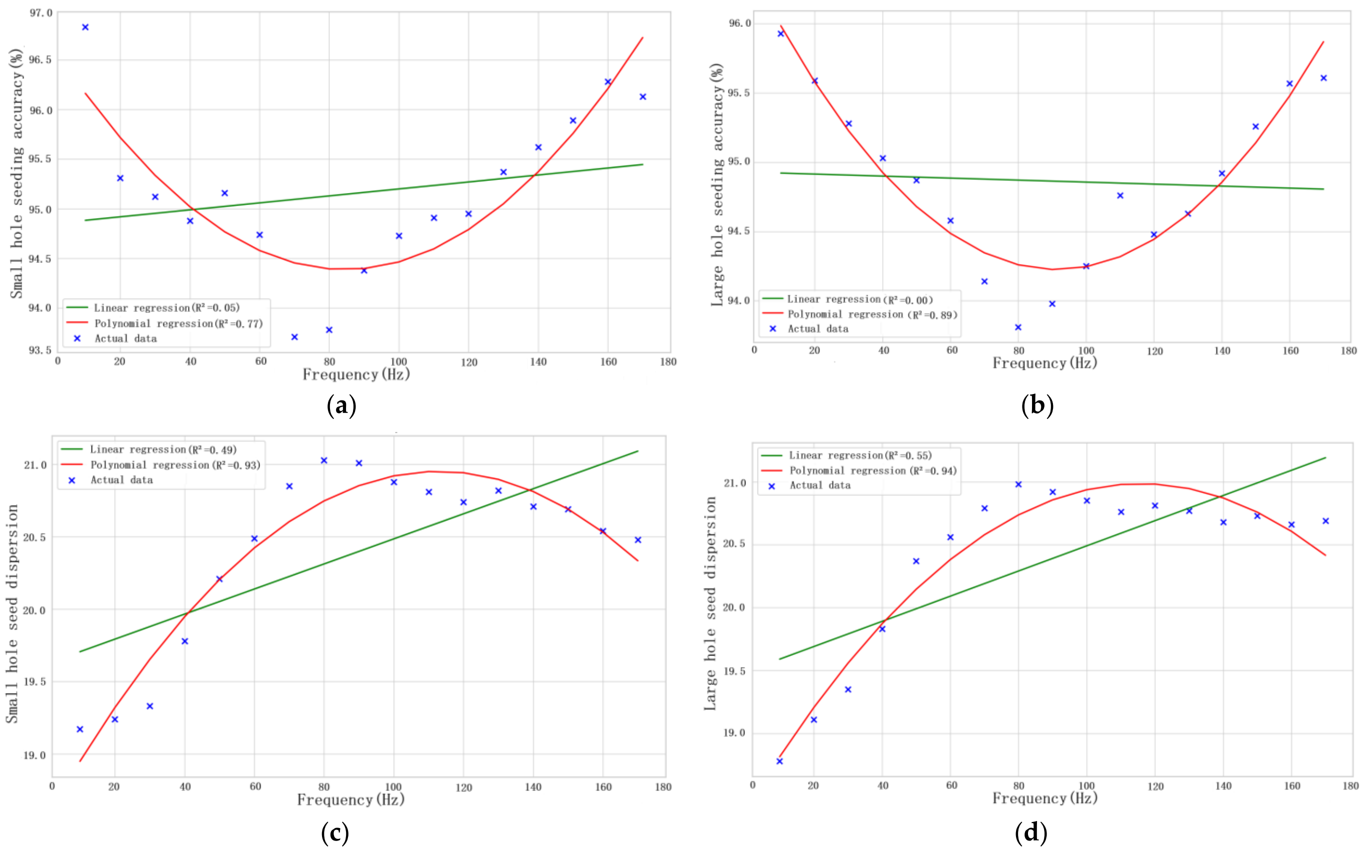

Figure 11. Regression analysis between vibration frequency of seed displacer and seeding accuracy and dispersion: (**a**) small hole seeding accuracy, (**b**) large hole seeding accuracy, (**c**) small hole seed dispersion, (**d**) large hole seed dispersion.

A comprehensive analysis revealed a substantial influence of vibration frequency on the performance of the planter seed discharger, with mid-frequency vibrations notably exerting a pronounced negative effect on both the seeding accuracy and dispersion. These findings offer crucial insights for the strategic design of the seeder and power chassis structure. This underscores the importance of considering performance variations across different frequencies in the design phase of both the power chassis and seeder, particularly emphasizing the need for refined vibration control within the mid-frequency range. This underscores the significance of optimizing the suspension systems of the power chassis and engine to suit diverse vibration environments, ultimately enhancing seeding efficiency and quality.

5. Conclusions

(1) This study meticulously examined the 2BDXZ-10CP(20) rice precision hole seeder, focusing on the vibrational dynamics encountered under various sowing conditions. Time-domain analysis of the vibrational signals indicated that the seeder experienced higher levels of overall vibration in sandy-loam soil when compared to those encountered in clay-loam soil field operations. Notably, an increase in the forward speed of the seeder correlated with heightened vibration acceleration. Additionally, under consistent operating speeds and soil conditions, the root mean square (RMS) vibration value of the seed dispenser within the seeder was observed to exceed that of the initial dispenser configuration. This finding suggests a direct transmission of vibrational energy from the power chassis to the seed dispenser, affecting its performance across different locations of the seeder.

(2) Frequency domain analysis revealed that the operational vibrations associated with the seeder predominantly fell within the 0 to 170 Hz range, a characteristic that held true across both clay loam and sandy loam fields, irrespective of variations in the forward speed of the seeder's power chassis. The factors primarily influencing this frequency distribution included the engine speed of the power chassis in paddy fields, the rotational speed of the power take-off (PTO) rotary ploughing device, and external stimuli from varied operational environments.

(3) Through the establishment of a vibration test bed, our research conclusively demonstrated that vibration frequency significantly influenced the seeding accuracy and dispersion of the seeder, with pronounced effects observed within the 70–130 Hz frequency range. During this interval, a noticeable decline in seeding accuracy and an increase in seed dispersion were observed, likely attributable to vibrational instability and resonance phenomena within the seeder's mechanical components. Conversely, as the frequency escalated to the 140–170 Hz range, there was a marked restoration in seeding accuracy and a deceleration in the rate of dispersion increase. This trend reversal suggests a diminished impact of high-frequency vibrations on the mechanical integrity of the seeder. The observed slowdown in dispersion increase within the higher frequency domain underscores the potential mitigating effects of high-frequency vibrations on the mechanical framework of the seeder. Furthermore, analysis via a polynomial regression model revealed that the variations in seeding performance could not be encapsulated by a straightforward linear relationship. Instead, these variations were likely influenced by a multitude of factors, including the mechanical response characteristics of the seeder and the operational complexities of the power chassis. This complexity hints at the necessity for further in-depth investigations to unravel the intricate interplay of these contributing factors and their collective impact on the seeder's performance.

Author Contributions: Conceptualization, D.Y., F.P., Z.Z., M.Z., W.Y., Y.Z., J.H., Y.H., W.Z., Y.W., Z.G., J.L., G.L., X.Q. and Z.W.; methodology, D.Y., Z.Z. and F.P.; software, D.Y. and F.P.; validation, F.P., Z.Z., G.L., X.Q. and Y.H.; investigation, D.Y. and Z.W.; writing—original draft preparation, D.Y., J.L., Y.W., Y.H. and F.P.; writing—review and editing, D.Y., J.H., Y.Z., M.Z. and W.Y.; formal analysis, D.Y., W.Z. and F.P.; investigation, Y.W. and Z.G.; supervision, J.H., Y.Z. and M.Z.; project administration, Z.W. and J.H.; funding acquisition, Z.W. All authors have read and agreed to the published version of the manuscript.

Funding: National Natural Science Foundation of China (Grant No. 32171903), Guangdong Basic and Applied Basic Research Foundation (Grant No. 2020B1515020034), supported by the earmarked fund for CARS (Grant No. CARS-01).

Institutional Review Board Statement: Not applicable.

Data Availability Statement: The data reported in this study are contained within the article.

Acknowledgments: We would like to express our gratitude to our supervisor for their project funding support and guidance on this paper, as well as to our fellow researchers for their help and support.

Conflicts of Interest: The authors declare no conflicts of interest.

References

1. Luo, X.W.; Liao, j.; Hu, L.; Zang, Y.; Zhou, Z. Improving agricultural mechanization level to promote agricultural sustainable development. *Trans. Chin. Soc. Agric. Eng.* **2016**, *32*, 1–11.
2. Mahajan, G.; Chauhan, B.S.; Gill, M.S. Dry-seededrice culture in Punjab State of India: Lessons learned from farmers. *Field Crops Res.* **2013**, *144*, 89–99. [CrossRef]
3. Kumar, V.; Ladha, J.K. Direct seeding of rice: Recent developments and future research needs. *Adv. Agron.* **2011**, *111*, 297–413.
4. Yang, L.; Yan, B.X.; Zhang, D.X. Research progress on precision planting technology of maize. *Trans. Chin. Soc. Agric. Mach.* **2016**, *47*, 38–48.
5. Mishra, A.K.; Khanal, A.R.; Pede, V.O. Is direct seeded rice a boon for economic performance? Empirical evidence from India. *Food Policy* **2017**, *73*, 10–18. [CrossRef]
6. Luo, X.W.; Wang, Z.M.; Zeng, S. Recent advances in mechanized direct seeding technology for rice. *J. South China Agric. Univ.* **2019**, *40*, 1–13.
7. Rao, A.N.; Brainard, D.C.; Kumar, V.; Ladha, J.K.; Johnson, D.E. Preventive weed management in direct-seeded rice: Targeting the weed seedbank. *Adv. Agron.* **2017**, *144*, 45–142.
8. Bhushan, L.; Ladha, J.K.; Gupta, R.K.; Singh, S.; Saharawat, Y.; Gathala, M.; Pathak, H.; Tirol-Padre, A. Saving of water and labor in a rice-wheat system with no-tillage and direct seeding technologies. *Agron. J.* **2007**, *99*, 1288–1296. [CrossRef]
9. Weerakoon, W.M.W.; Mutunayake, M.M.P.; Bandara, C.; Rao, A.; Bhandari, D.; Ladha, J. Direct-seeded rice culture in Sri Lanka:Lessons from farmers. *Field Crops Res.* **2011**, *121*, 53–63. [CrossRef]
10. Pandey, S.; Mortimer, M.; Wade, L.; Tuong, T.P.; Lopez, K.; Hardy, B. *Direct Seeding: Research Issues and Opportunities*; International Rice Research Institute (IRRI): Los Banos, Philippines, 2002; pp. 3–14.
11. Pandey, S.; Velasco, L. *Rice Is Life: Scientific Perspectives for the 2lst Century*; Copyright International Rice Research Institute: Tsukuba, Japan, 2005; pp. 178–181.
12. Zheng, G.J.; Tao, Y.; Shen, X.L.; Ye, C.; Xu, Y.; Chu, G.; Xu, C.; Wang, D. Study on Rice Seed Germination and Seedling Emergence and Related Problems in Direct Seeding Production. *China Rice* **2023**, *29*, 49–55.
13. Chen, X.F.; Tang, Y.P.; Xie, Y.J.; Li, S.; Chu, J.; Ao, F.; Peng, W.; Li, H.S.; Wan, Y. Research Advances of Rice Mechanical Direct-seeding Technology in China. *China Rice* **2018**, *24*, 9–15.
14. Wang, Z.M.; Pei, J.; He, J. Development of the sowing rate monitoring system for precision rice hill-drop drilling machine. *Trans. Chin. Soc. Agric. Eng.* **2020**, *36*, 9–16.
15. Yang, Y.P. *Design and Experimental Research on Seeder of Rice Dry Field Direct Seeding Planter*; Qingdao University of Technology: Qingdao, China, 2021.
16. Wang, Z.M. *Research and Experiment on Key Technology of Rice Direct Seeding Machine Rice Direct Seeding Machine*; Hubei University of Technology: Wuhan, China, 2020.
17. Liao, Y.T.; Qi, T.X.; Liao, Q.X.; Zeng, R.; Li, C.L.; Gao, L.P. Vibration characteristics of pneumatic combined precision rapeseed seeder and its effect on seeding performance. *J. Jilin Univ. (Eng. Technol. Ed.)* **2022**, *52*, 1184–1196.
18. Wang, Q.; Zhu, L.T.; Li, M.W.; Huang, D.Y.; Jia, H.L.; Zhuang, J. Vibration characteristics of corn no-tillage finger-type precision planter and its effect on seeding performance. *Trans. Chin. Soc. Agric. Eng.* **2019**, *35*, 9–18.
19. Gu, L.C.; Guo, L.; Li, H. Analysis of the vibration characteristics of three-point-hanging shovel type wheat planter frame. *Jiangsu Agric. Sci.* **2017**, *45*, 214–216.
20. Xu, L.Z.; Li, Y.M.; Sun, P.P. Vibration measurement and analysis of tracked-whole feeding rice combineharvester. *Trans. Chin. Soc. Agric. Eng.* **2014**, *30*, 49–55.
21. Far, J.J.; Upadhyaya, S.K. Development and field evaluation of a hydropneumatic planter for primed vegetable seeds. *Trans. ASAE* **1994**, *37*, 1069–1072.
22. Mf, K.; Lan, Y.; Chen, C.; Smith, J.A. Opto-electronic sensor system for rapid evaluation of planter seed spacing uniformitly. *Trans. ASAE* **1998**, *41*, 237–245.
23. Niyamapa, T.; Salokhe, V.M. Force and pressure distribution under vibratory tillage tool. *J. Terramechanics* **2000**, *37*, 139–150. [CrossRef]
24. Vu, L.; Zhang, X.; Walton, O.R. A 3-D discrete-element method for dry granular flows of ellipsoidal particles. *Comput. Methods Appl. Mech. Eng.* **2000**, *187*, 483–528.
25. Min, Y.B.; Kim, S.T.; Kwon, H.D.; Moon, S.W.; Kang, D.H. Effect of the seed hopper vibration on the seeding performance of the vacuum suction nozzle seeder. *J. Biosyst. Eng.* **2008**, *33*, 179–185.
26. Yu, D.Y.; He, J.F.; Peng, F.H.; Qian, C.; Zang, Y.; Zhang, M.; Yang, W.; Zeng, G.; Chen, J.; Qin, W.; et al. Study on Vibration Characteristics of Paddy Power Chassis under Different Driving Conditions. *Agriculture* **2023**, *13*, 1842. [CrossRef]
27. Gao, Z.P.; Xu, L.Z.; Li, Y.M.; Wang, Y.; Sun, P. Vibration measure and analysis of crawlertype rice and wheat combine harvester in field harvesting condition. *Trans. CSAE* **2017**, *33*, 48–55.

28. Xi, X.B.; Gao, W.J.; Gu, C.J.; Shi, Y.; Han, L.; Zhang, Y.; Zhang, B.; Zhang, R. Optimisation of no-tube seeding and its application in rice planting. *Biosyst. Eng.* **2021**, *210*, 115–128. [CrossRef]
29. Zhao, J.; Xi, X.B.; Shi, Y.J.; Zhang, B.; Qu, J.; Zhang, Y.; Zhu, Z.; Zhang, R. An Online Method for Detecting Seeding Performance Based on Improved YOLOv5s Model. *Agronomy* **2023**, *13*, 2391. [CrossRef]